Sea-level fingerprint of continental water and ice mass change from GRACE

Riccardo E. M. Riva,[1,2] Jonathan L. Bamber,[3] David A. Lavallée,[1] and Bert Wouters[4]

Received 22 July 2010; revised 17 August 2010; accepted 23 August 2010; published 12 October 2010.

[1] The Gravity Recovery and Climate Experiment satellites (GRACE) provide, for the first time, a method to directly measure mass exchange between the land and oceans over time. The dominant components of this exchange are due to continental ice loss/gain and land hydrology. Here, we determine the secular trend in these two components during the GRACE measurement era: 2003–2009. For each component, we model the distinct regional signatures or fingerprints of relative sea-level (RSL) change, obtaining maxima at low latitudes between ±40° N/S, but with particularly strong regional patterns. We estimate that the total ice and water mass loss from the continents is causing global mean sea-level to rise by 1.0 ± 0.4 mm/yr. Isolating the ice and hydrological signals, we find that the former is the sole net contributor to the global mean, while the latter dominates regional RSL changes in many coastal areas. **Citation:** Riva, R. E. M., J. L. Bamber, D. A. Lavallée, and B. Wouters (2010), Sea-level fingerprint of continental water and ice mass change from GRACE, *Geophys. Res. Lett.*, *37*, L19605, doi:10.1029/2010GL044770.

1. Introduction

[2] A sea-level fingerprint is the characteristic signature of sea-level changes due to a specific mass source. It identifies both the source location and magnitude. Fingerprints can be forward modelled by solving the sea-level equation [*Farrell and Clark*, 1976], which describes the interaction between sea-level changes and solid earth deformation, coupled through gravitation. The sea-level equation solves for the equilibrium configuration of a passive ocean, i.e., an ocean whose surface at rest represents an equipotential surface of the gravity field. Since sea-level changes represent a global phenomenon, only an accurate constraint on global mass exchange between continents and ocean can be used to compute fingerprints. The possibility of such a global constraint on surface mass transport is presented by satellite gravimetry measurements, in particular those provided by the GRACE mission [*Tapley et al.*, 2004], due to their high temporal and spatial resolution.

[3] Here, we use GRACE gravity measurements to model continental trends in surface mass, and subsequently use the sea-level equation to determine RSL changes. The resulting fingerprint is complementary to independent observations of sea-level due to changes in ocean mass, such as bottom pressure gauges, or ocean volume from satellite altimetry or tide gauges.

2. Datasets and Methodology

2.1. GRACE Data

[4] The appearance of vertical stripes in the monthly gravity fields obtained from GRACE requires the post-processing use of dedicated filters [*Swenson and Wahr*, 2006; *Wouters&Schrama*, 2007; *Klees et al.*, 2008]. In this study, we make use of the DEOS Mass Transport release 1 fields (DMT-1) [*Liu et al.*, 2010], which are filtered by means of an anisotropic non-symmetric filter [*Klees et al.*, 2008]. The applied filter maximizes the signal-to-noise ratio and is therefore "optimal" in a statistical sense: as a result, the DMT-1 fields are almost free from spatially correlated noise and particularly suited for fingerprinting studies. The available dataset consists of 6 years of monthly solutions, from February 2003 through February 2009, computed in the spherical harmonic domain up to degree and order 120. By a least square approach, we have obtained a linear trend on a 0.5°x0.5° grid, estimated simultaneously with four periodic signals (annual, semi-annual, S2- and K2-tide). For error estimation purposes, we also use the Center for Space Research (CSR) Release-04 fields [*Bettadpur*, 2007], filtered by means of Empirical Orthogonal Functions (EOF) [*Wouters and Schrama*, 2007].

2.2. GIA Model

[5] Here, glacio-isostatic adjustment (GIA) represents the ongoing deformation of the Solid Earth due to changes in surface load during the last glacial cycle, where the effect of the large mass exchange between the continents and the oceans is still visible today because of the delayed response of the visco-elastic Earth. In particular, GIA is causing changes in the shape and the rotation of the earth, as well as RSL changes. GIA depends on reconstructions of the glacial history and on the parameterization of the solid Earth, both of which possess significant uncertainties, mainly because of the limited availability of direct evidence. For this study, we use a widely adopted model of ice history and Earth viscosity, namely ICE-5G (VM2) [*Peltier*, 2004], and we include the effect of earth rotation [*Milne and Mitrovica*, 1998]. For the contribution of Antarctica, we use the ice history model IJ05 [*Ivins and James*, 2005], in combination with an Earth model with a higher viscosity in the lower mantle (10^{22} Pa s) and a thinner elastic lithosphere (60 km) than VM2 [*Riva et al.*, 2009]. Antarctica only contributes about 10% of global sea-level rise since the last glacial maximum. Thus, the use of IJ05 instead of ICE-5G is

[1]DEOS, Delft University of Technology, Delft, Netherlands.
[2]Faculty of Geosciences, Utrecht University, Utrecht, Netherlands.
[3]Bristol Glaciology Centre, School of Geographical Sciences, University of Bristol, Bristol, UK.
[4]Royal Netherlands Meteorologic Institute, De Bilt, Netherlands.

0094-8276/10/2010GL044770

important, primarily, at the regional scale and has a minor effect on the global GIA signal. In order to account for the stabilizing effect of the non-hydrostatic ellipticity of the Earth on polar motion [*Mitrovica et al.*, 2005], we scale our prediction of true polar wander (TPW) to half its original value, obtaining a polar motion of about 0.7 deg/Myr. There is still an open debate about many aspects of the last glaciation, as well as on the relative importance of various earth processes with respect to global GIA [*Ivins and Wolf*, 2008, and references therein]. Our approach, where we use a "standard" model, is designed to separate GIA issues from the fingerprinting problem, while maintaining the reproducibility of our results. However, we accept that limitations in the representation of GIA exist (we estimate the GIA uncertainty in global mass exchange to be about 20%).

2.3. Leakage Correction

[6] The combined effect of the flight altitude of the GRACE satellites and the accuracy of the on-board K-band ranging instruments sets an upper limit to the measurement resolution of about 300 km. This causes a problem when mass changes have to be constrained within a given basin that is of a comparable scale. A possible solution makes use of averaging kernels in combination with appropriate scaling factors [e.g., *Velicogna and Wahr*, 2006]. However, the determination of a scaling factor can be problematic for large regions, where the mass budget is resulting from the contribution of both positive and negative signals that have an anisotropic spatial pattern. An alternative approach is to expand the size of the basin to include a buffer zone that has a width controlled by the GRACE resolution. This approach is based on the assumption that most of the leakage is directed outwards, which is usually the case when the basin boundaries are represented by coastlines. It is analogous to the use of a modified ocean kernel proposed by *Chambers et al.* [2007], who were looking for the complementary signal (ocean mass change) and suggested discarding changes occurring within 300 km from the coast. The use of a buffer zone is sufficient to determine the land mass budget. However, for the purpose of modelling RSL fingerprints, we need to physically locate the mass changes over land. To this end, we isolate the signal inside the buffer zone (represented by the first 250 km of ocean around land) and, by means of a convolution filter, we force it to leak back over land. Before adding this "leaked" buffer to the land load, we restore its original mass content through scaling. For the convolution, we use a boxcar filter with a half-width equal to the width of the buffer zone, to concentrate the signal in coastal areas. For the scaling, we use a fixed factor of 3, where this value has the following geometrical explanation: if the signal within the buffer were flat, then the appropriate scaling factor would be 4 (1/2 of the signal would remain within the buffer zone and 1/4 of it would be spread at each side); if the signal were concentrated very close to the coastline, then the scaling factor would be 2 (1/2 of the signal would remain over the ocean and 1/2 over land); so, since the land leakage decreases from the coast outwards, the scaling factor needs to be between 2 and 4. The average value of 3 is appropriate when the buffer width is comparable to the resolution limit. This leakage correction has the advantage of being easily implemented for all continents at once, since the scaling factor is determined a priori. It provides an approximated correction, but it also reduces the leakage from the oceans onto land, since a scaling factor smaller than 4 gives more weight to that part of the signal closer to the coast. We apply only two exceptions to this procedure: around Sumatra, where we do not use any buffer to limit contamination due to the co- and post-seismic deformation of the 2004 earthquake, and the Antarctic Peninsula, where we have increased the scaling factor to the empirical value of 7.5 to account for the fact that leakage is larger than normal due to the small land width (this empirical value has been obtained by forcing the load restored over land to be equal to the original mass content of the buffer zone). The total effect of the leakage correction is to increase our estimate of the average continental mass change by 40%, where this value is only marginally dependent on the filter width (in the range 150–350 km), since the pre-determined scaling factor effectively reduces ocean leakage.

2.4. Determination of the Land Load

[7] The gravity changes measured by GRACE are the result of dynamic processes taking place inside the Earth and within its surface (water+atmosphere) layer. The largest signal due to the solid Earth is GIA, discussed above. As far as the surface layer is concerned, this can be separated into several components: continental water (surface and ground water, soil moisture, snow and ice), the passive ocean (in gravitational equilibrium), the dynamic ocean and the atmosphere. Mass changes over land and mass changes from the passive ocean are directly connected through gravitational attraction; in order to accurately determine land mass changes, the passive ocean response has to be taken into account. We work under the assumption that the dominant signal in the multi-annual ocean trend is due to gravitational effects rather than ocean dynamics. This is a reasonable assumption, especially for the lowest harmonic degrees that will be highly sensitive to large-scale mass transport. Our approach follows the philosophy of *Clarke et al.* [2005] and is based on the consideration that the gravity signal over land as measured by GRACE is contaminated by the gravitational signature of the passive ocean. Iteratively, we determine a different land load that, once combined with the elastic response of the Earth and a passive ocean (through the sea-level equation), produces the same gravity signal over land as observed by GRACE. Our iterative approach is as follows:

[8] 1. After correcting the filtered GRACE trend field for GIA and leakage, and after restoring the atmospheric and ocean products (AOD1B) removed during the GRACE processing, we determine the initial land load by computing the surface mass change in terms of equivalent water height [*Wahr et al.*, 1998] and multiplying the resulting field by a land kernel (exact at 0.5°x0.5° resolution).

[9] 2. We use this land load as the input load for the sea-level equation and determine the equilibrium load (up to degree and order 360, while conserving mass and including the effect of earth rotation).

[10] 3. We take the difference between the equilibrium load and the initial land load and we add it to the input load, obtaining an updated land load.

[11] 4. We iterate from (ii) until the equilibrium load converges (in practice, about three iterations are enough to obtain convergence within one percent).

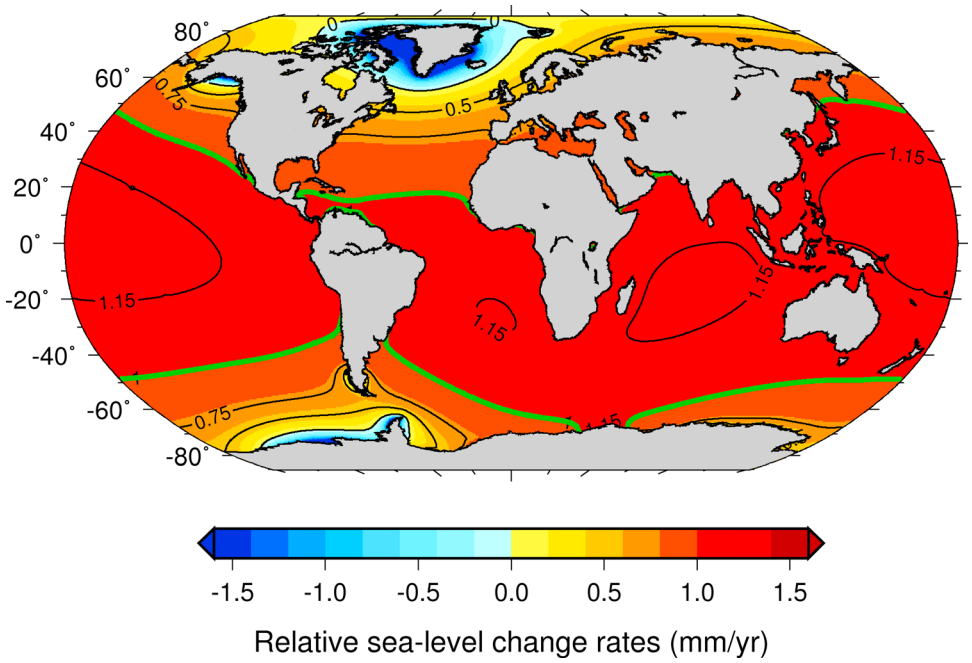

Figure 1. GRACE RSL fingerprint, solely due to the contribution of continental ice (green contour: eustatic equivalent, 1 mm/yr).

[12] As far as the ocean is concerned, we implicitly fit its passive component and consider as noise the part of the signal due to dynamic processes, that must have a zero mean. Through this approach, we also improve the determination of the degree 1 component of the load (see Table S1 of the auxiliary material for the resulting geocenter motion), which cannot be directly observed by GRACE and needs to be constrained by means of additional datasets [*Swenson et al.*, 2008] or consistency relations [*Clarke et al.*, 2005].[1] The final land load is globally larger in magnitude by about 16% (the degree 1 component increases by 60%) and has a different configuration from the initial load, because the passive ocean affects both the size and the spatial distribution of the surface mass estimate (Figure S1).

3. Results and Error Estimates

[13] In Figure 1, we show the RSL fingerprint solely due to the major glaciated regions (Greenland, Iceland, Svalbard, Arctic Canada, Alaska, Patagonia and Antarctica). We obtain this fingerprint by applying a mask that only preserves the glaciated regions to the land load determined above, after removing the atmosphere-ocean trend, and using this ice load as input for the sea-level calculations. A green contour indicates the eustatic sea-level change (equal to 1.0 ± 0.2 mm/yr). At latitudes above this, RSL changes are less than the global average and vice versa for lower latitudes. Since these mass sources are concentrated in polar regions, the pattern of RSL change is rather smooth, with a large drop in the near-field and the largest rise concentrated below ~ ±40° N/S, with a peak value of almost 1.2 mm/yr in the Western Pacific. In Figure 2, we show our full GRACE fingerprint, where the land load covers all the continental areas and includes the atmosphere-ocean trend. The eustatic equivalent is 1.0 ± 0.4 mm/yr, in agreement with the values obtained by *Leuliette and Miller* [2009] (0.8 ± 0.5 mm/yr) for a shorter time-span (2004–2007). The net impact of land hydrology on the global ocean mass balance is slightly negative and amounts to −0.1 ± 0.3 mm/yr. In spite of its negligible impact on the mean mass trend, multi-annual variations in land hydrology (Figure 3) largely dominate regional RSL changes in coastal areas. A significant amplification of the average RSL rise is observed at many locations, such as Eastern Canada, central South America, India and most of Northern Eurasia, with peak values around 1.5 mm/yr and a relative increase locally larger than 100%. Those regions are retaining water, which in turn causes local RSL to rise due to gravitational attraction. Conversely, in many other regions, drought partially compensates for the effects of global sea-level rise, such as around the Eastern US, Argentina, most of Oceania and South-East Asia.

[14] To estimate the GIA error, we use ICE-5G in combination with different values of lower mantle viscosity and with the IJ05 ice history for Antarctica, obtaining a mean uncertainty of 0.24 mm/yr for the global budget (corresponding to about 20% of the total GIA signal) and 0.10 mm/yr for the ice sources alone. For GRACE over glaciated regions, we use the mean trend uncertainty of 0.10 mm/yr. We also compute the difference between DMT-1 and CSR fields as a measure of the uncertainty between different GRACE solutions, obtaining an additional uncertainty of 0.13 mm/yr and hence a total GRACE error of 0.16 mm/yr. For the global GRACE estimate, for which the mean trend error would be too conservative, we first compute the average continental mass change for each

[1] Auxiliary materials are available in the HTML. doi:10.1029/2010GL044770.

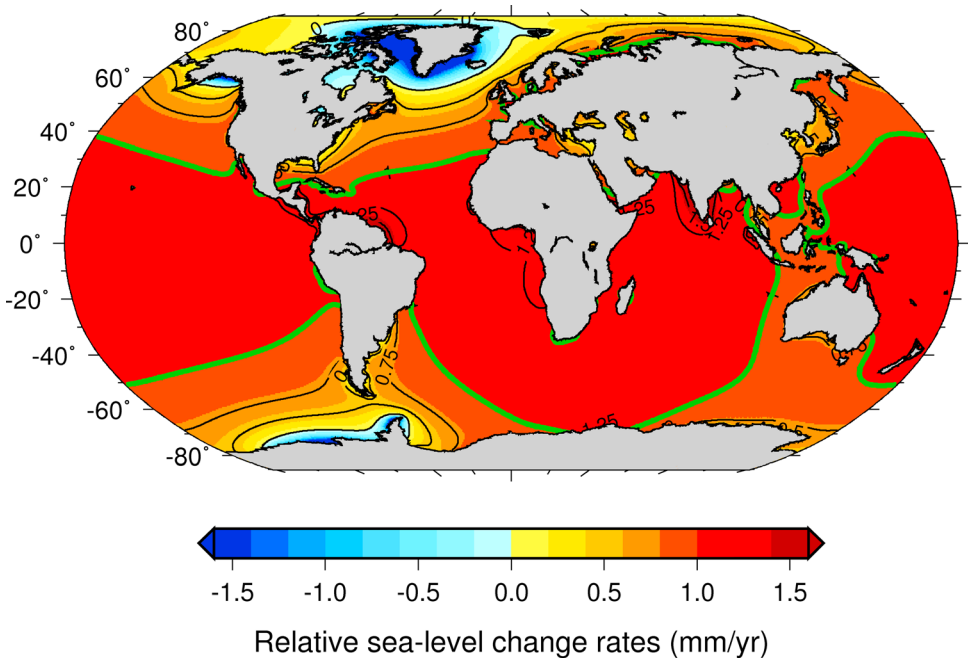

Figure 2. GRACE RSL fingerprint (green contour: eustatic equivalent, 1 mm/yr).

monthly solution, and then compute a new trend uncertainty of 0.22 mm/yr. The difference between DMT-1 and CSR fields provides an additional 0.18 mm/yr error, which leads to a total GRACE error of 0.28 mm/yr. Combining GRACE and GIA errors, the final mean uncertainties are: 0.37 mm/yr for the global estimate, 0.19 mm/yr for the ice contribution and 0.27 mm/yr for the hydrology contribution. We have verified the validity of our assumption of a passive ocean by computing the residual mean ocean mass trend (GRACE + AOD1B − GIA − equilibrium load), which was found to be at least an order of magnitude smaller than the mass budget uncertainty (Figure S2).

4. Discussion and Conclusions

[15] The fingerprints that we have shown represent forward models of RSL change due to the gravitational effect of surface mass redistribution. Since our estimate of the surface load is based on direct and global observations, they can be regarded as "observed" fingerprints. They have been

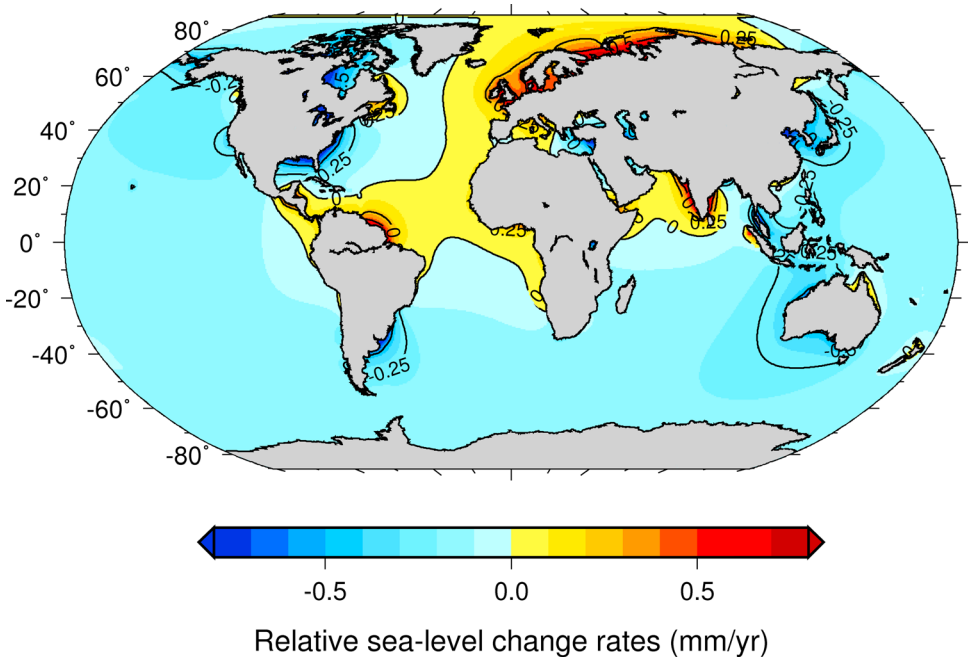

Figure 3. GRACE RSL fingerprint, solely due to the contribution of land hydrology.

obtained by assuming an equilibrium ocean with homogeneous density and are therefore complementary to models of steric sea-level changes (driven by temperature or salinity variations) and ocean dynamics. The result shown in Figure 2 represents the fingerprint of water exchange between continents and oceans for the period Feb.2003–Feb.2009. This is only six years and inter-annual variability in the strength of, for example, the Monsoon and seasonal rainfall over the Amazon basin are significant compared to the trends observed. The regional fingerprint of land hydrology may, therefore, look different for a longer time interval. This is not the case for the continental ice fingerprint shown in Figure 1. In this case, the longer-term secular trends are dominant [*Meier et al.*, 2007; *Rignot et al.*, 2008; *van den Broeke et al.*, 2009]. This fingerprint is linearly scalable with the magnitude of the mass fluxes, which have been accelerating during the last ~decade or more [*Meier et al.*, 2007; *Velicogna*, 2009]. Furthermore, unlike the RSL impact of ocean dynamics, the land ice signal is cumulative over time and, unlike the steric signal, the pattern is stationary in space, as long as the relative source contributions do not change significantly [*Tamisiea et al.*, 2001]. Thus, if Antarctica and Greenland continue to lose mass at the current rate, then all regions at low latitude will experience a gravitationally driven RSL increase that is around 20% greater than the average value. The effect of land hydrology (Figure 3) is locally relatively large and, at low latitudes, dominant compared to the ice signal, which is important for studies based on local RSL measurements, such as tide gauges. However, this pattern is driven by very large inter-annual variability in precipitation and evaporation rather than a secular trend and its magnitude and spatial pattern will, therefore, reduce and change over longer time scales. Moreover, this fingerprint will be affected by variations in the amount of water impounded behind dams [*Fiedler and Conrad*, 2010].

[16] The estimate of land ice mass loss obtained from GRACE is significantly smaller than those based on glaciological constraints [*Meier et al.*, 2007; *van den Broeke et al.*, 2009]. This is partially due to the limited resolution of GRACE and to the use of filters, but also to the large uncertainties in the glaciological estimates, based on a combination of different techniques and on a generally non-uniform sampling (spatial and temporal). Moreover, our estimate of glacier mass loss does not account for the contribution of the Rocky Mountains and Himalayas, due to the local signal contamination by land hydrology. As far as different GRACE solutions are concerned, the comparison between DMT-1 and CSR fields (Figure S3) shows fairly good agreement: in particular, the global mass balance and the fingerprint due to the ice sources are very similar, while the largest differences concern the regional impact of land hydrology.

[17] Finally, our results are also dependent on the adopted GIA model, which carries uncertainties in both the ice history and the earth parameterization. In particular, uncertainties in the value of lower mantle viscosity affect the spherical harmonic degree 2 component of the signal, which controls a large part of the mass exchange between polar and equatorial regions, as well as earth rotation: this is reflected in the uncertainty in the global mass budget and in the exact location and amplitude of the equatorial maxima in the RSL fingerprints. Uncertainties in the glaciation-deglaciation history and in the parameterization of the shallower part of the Earth (upper mantle and lithosphere) will mostly affect regional RSL changes at higher latitudes and estimates of the Antarctic ice sheet mass balance [*Horwath and Dietrich*, 2009]. Conversely, regional RSL changes in coastal areas and away from the former ice sheets, that are controlled by surface mass transport over neighbouring regions, are rather independent of the applied GIA correction.

References

Bettadpur, S. (2007), GRACE 327-734 level-2 gravity fields product user handbook, *CSR Publ. GR-03-01*, 19 pp., Univ. of Tex. at Austin, Austin.

Chambers, D. P., M. E. Tamisiea, R. S. Nerem, and J. C. Ries (2007), Effects of ice melting on GRACE observations of ocean mass trends, *Geophys. Res. Lett.*, *34*, L05610, doi:10.1029/2006GL029171.

Clarke, P. J., D. A. Lavallée, G. Blewitt, T. M. van Dam, and J. M. Wahr (2005), Effect of gravitational consistency and mass conservation on seasonal surface mass loading models, *Geophys. Res. Lett.*, *32*, L08306, doi:10.1029/2005GL022441.

Farrell, W. E., and J. A. Clark (1976), On postglacial sea level, *Geophys. J. R. Astron. Soc.*, *46*, 647–667, doi:10.1111/j.1365-246X.1976.tb01252.x.

Fiedler, J. W., and C. P. Conrad (2010), Spatial variability of sea level rise due to water impoundment behind dams, *Geophys. Res. Lett.*, *37*, L12603, doi:10.1029/2010GL043462.

Horwath, M., and R. Dietrich (2009), Signal and error in mass change inferences from GRACE: The case of Antarctica, *Geophys. J. Int.*, *177*, 849–864, doi:10.1111/j.1365-246X.2009.04139.x.

Ivins, E. R., and T. S. James (2005), Antarctic glacial isostatic adjustment: A new assessment, *Antarct. Sci.*, *17*(4), 541–553, doi:10.1017/S0954102005002968.

Ivins, E. R., and D. Wolf (2008), Glacial isostatic adjustment: New developments from advanced observing systems and modelling, *J. Geodyn.*, *46*, 69–77, doi:10.1016/j.jog.2008.06.002.

Klees, R., E. A. Revtova, B. C. Gunter, P. Ditmar, E. Oudman, H. C. Winsemius, and H. H. G. Savenije (2008), The design of an optimal filter for monthly GRACE gravity models, *Geophys. J. Int.*, *175*, 417–432, doi:10.1111/j.1365-246X.2008.03922.x.

Leuliette, E. W., and L. Miller (2009), Closing the sea level rise budget with altimetry, Argo, and GRACE, *Geophys. Res. Lett.*, *36*, L04608, doi:10.1029/2008GL036010.

Liu, X., P. Ditmar, C. Siemes, D. C. Slobbe, E. Revtova, R. Klees, R. Riva, and Q. Zhao (2010), DEOS Mass Transport model (DMT-1) based on GRACE satellite data: methodology and validation, *Geophys. J. Int.*, *181*, 769–788.

Meier, M. F., et al. (2007), Glaciers dominate Eustatic sea-level rise in the 21st century, *Science*, *317*(5841), 1064–1067, doi:10.1126/science.1143906.

Milne, G. A., and J. X. Mitrovica (1998), Postglacial sea-level change on a rotating Earth, *Geophys. J. Int.*, *133*, 1–9, doi:10.1046/j.1365-246X.1998.1331455.x.

Mitrovica, J. X., J. Wahr, I. Matsuyama, and A. Paulson (2005), The rotational stability of an ice-age earth, *Geophys. J. Int.*, *161*, 491–506, doi:10.1111/j.1365-246X.2005.02609.x.

Peltier, W. R. (2004), Global glacial isostasy and the surface of the ice-age Earth: The ICE-5G (VM2) model and GRACE, *Annu. Rev. Earth Planet. Sci.*, *32*, 111–149, doi:10.1146/annurev.earth.32.082503.144359.

Rignot, E., et al. (2008), Recent Antarctic ice mass loss from radar interferometry and regional climate modelling, *Nat. Geosci.*, *1*(2), 106–110, doi:10.1038/ngeo102.

Riva, R. E. M., et al. (2009), Glacial isostatic adjustment over Antarctica from combined ICESat and GRACE satellite data, *Earth Planet. Sci. Lett.*, *288*, 516–523, doi:10.1016/j.epsl.2009.10.013.

Swenson, S., and J. Wahr (2006), Post-processing removal of correlated errors in GRACE data, *Geophys. Res. Lett.*, *33*, L08402, doi:10.1029/2005GL025285.

Swenson, S., D. Chambers, and J. Wahr (2008), Estimating geocenter variations from a combination of GRACE and ocean model output, *J. Geophys. Res.*, *113*, B08410, doi:10.1029/2007JB005338.

Tamisiea, M. E., J. X. Mitrovica, G. A. Milne, and J. L. Davis (2001), Global geoid and sea level changes due to present-day ice mass fluctuations, *J. Geophys. Res.*, *106*(B12), 30,849–30,863, doi:10.1029/2000JB000011.

Tapley, B. D., S. Bettadpur, M. Watkins, and C. Reigber (2004), The gravity recovery and climate experiment: Mission overview and early results, *Geophys. Res. Lett.*, *31*, L09607, doi:10.1029/2004GL019920.

van den Broeke, M., et al. (2009), Partitioning recent Greenland mass loss, *Science*, *326*(5955), 984–986, doi:10.1126/science.1178176.

Velicogna, I. (2009), Increasing rates of ice mass loss from the Greenland and Antarctic ice sheets revealed by GRACE, *Geophys. Res. Lett.*, *36*, L19503, doi:10.1029/2009GL040222.

Velicogna, I., and J. Wahr (2006), Measurements of time-variable gravity show mass loss in Antarctica, *Science*, *311*, 1754–1756, doi:10.1126/science.1123785.

Wahr, J., M. Molenaar, and F. Bryan (1998), Time variability of the Earth's gravity field: Hydrological and oceanic effects and their possible detection using GRACE, *J. Geophys. Res.*, *103*, 30,205–30,229, doi:10.1029/98JB02844.

Wouters, B., and E. J. O. Schrama (2007), Improved accuracy of GRACE gravity solutions through empirical orthogonal function filtering of spherical harmonics, *Geophys. Res. Lett.*, *34*, L23711, doi:10.1029/2007GL032098.

J. L. Bamber, Bristol Glaciology Centre, School of Geographical Sciences, University of Bristol, University Road, Bristol BS8 1SS, UK.

D. A. Lavallée and R. E. M. Riva, DEOS, Delft University of Technology, Delft, Kluyverweg, NL-2629 HS Netherlands. (r.e.m.riva@tudelft.nl)

B. Wouters, Royal Netherlands Meteorologic Institute, Postbus 201, NL-3730 AE De Bilt, Netherlands.